Detection of Negative Online Public Opinion among College Students Based on Sooty Tern Optimization Algorithm and Dissemination Trend Data

Kaiying Zhu
Railway Locomotive and Rolling Stock College, Jilin Railway Technology College, Jilin 132299, China
Email of corresponding author: zhukaiying_jlrtc@163.com

Keywords: Sooty tern optimization algorithm; Communication trends; Online public opinion; Support vector machine; Elman neural network

Received: June 11, 2024

Under the background of rapid advancement of information technology and the Internet, the impact of online public opinion on social stability and campus environment is increasingly significant, especially the negative online public opinion involving college students. To effectively detect and manage negative online public opinion, this study proposes a public opinion classification model that combines the Sooty Tern algorithm with support vector machines. The traditional Sooty Tern optimization algorithm is improved by using three strategies: Tent chaotic mapping, adaptive t-distribution mutation factor, and random walk. Combining it with neural network, a public opinion prediction model with time series characteristics is designed. The test results showed that the classification model had a precision rate of 92.86%, a recall rate of 93.75%, an F1 value of 93.82%, a resource consumption rate of 18.63%, and an average calculation time of 9.1s, which is the best among the comparison models. In addition, the classification accuracy of the model for current affairs, economy, culture, and social public opinion categories was 94.33%, 96.24%, 94.89%, and 98.98%, respectively. In terms of prediction accuracy, when the target error value was 0.5, the average training times of the prediction model was only 49 times, and the average error value of the model was 0.1853. When the target error value was 0.1, the model was trained an average of 94 times and the average error value was 0.0725. The experiment shows that the detection system can quickly identify and locate negative public opinion in large-scale data, and accurately predict its dissemination trend, providing a new warning information and response strategy for relevant management departments.

Povzetek: Študija uvaja model za zaznavanje negativnega spletnega mnenja med študenti s kombinacijo Sooty Tern optimizacijskega algoritma in SVM, s tem pa učinkovito napoveduje trend širjenja negativnih mnenj.

1 Introduction

The process of the information society has made the internet an important component of people's daily life and social interaction, especially among college students who have a high usage rate and a wide coverage area [1-2]. Due to the popularity of social media and online platforms, the use of the internet as a medium by college students to obtain information, express opinions, and participate in social activities has become the mainstream trend [3]. However, this also brings new challenges to the management of Negative Online Public Opinion (NOPO). Negative Public Opinion (NPO) involving college students, such as inappropriate speech, false information, and online violence, poses a huge threat to their mental health, campus harmony, and social stability [4]. College students are particularly vulnerable to the adverse effects of NOPO due to their developmental stage, susceptibility to peer influence, and high engagement with social media platforms. The impact of NOPO can lead to severe consequences, including increased stress, anxiety, depression, and even suicidal tendencies among students. Moreover, the spread of such negative sentiments can disrupt the educational environment, affecting the overall academic performance and well-being of the student community [5]. To address the aforementioned challenges, numerous researchers have explored advanced algorithms and technologies aimed at improving the efficiency and accuracy of Online Public Opinion (OPO) management. In this context, the Sooty Tern Optimization Algorithm (STOA) has gradually gained widespread attention and demonstrated its application potential in multiple fields due to its superior global search ability and adaptability. STOA demonstrates remarkable global search capacity and adaptability, and has been extensively utilized in the domains of engineering optimization, machine learning, and data science. B. Muthazhagan et al. proposed a new STOA for image examination in lung cancer. This algorithm first used image segmentation techniques to

segment the denoised X image, and then used deep learning techniques to extract the structural features of nodules and enhance the texture features of the image. Finally, it applied STOA to distinguish between normal small cell lung cancer and cancer from X-ray images [6]. J. Wang et al. established a nonlinear optimization mathematical model for Mine Ventilation (MV) network to reduce energy consumption of MV system, and proposed an improved STOA based on this model. The model adopted uniform reverse, fitness distance balance selection, and mutation strategies to optimize the algorithm, which could reduce the total energy usage amount of the mine by about 35.06% [7]. H. Jia et al. proposed a hybrid model based on STOA to perfect the Support Vector Machine (SVM) and recognize the optimal feature set for effective data preprocessing. The hybrid model combined the STOA and differential evolution to rise search efficacy and convergence velocity. It has been proven to have good recognition performance in experimental tests on 12 datasets [8]. J. He et al. proposed an improved STOA to address the difficulty in finding the global optimal solution. This algorithm combined multiple search guidance approaches and location update modes, designing average individuals and randomly selected individuals to instruct the search. They also proposed 6 position update modes, including an enhanced scaling mode with extended spiral radius and 5 other modes built on offset operation [9]. J. Zhang et al. proposed an optimized Variational Mode Decomposition (VMD) fault diagnosis method based on STOA to address the problem of difficult identification of fault characteristics in planetary gearbox vibration signals. This approach first utilized STOA to optimize the VMD parameters, then decomposed the signal using the VMD method, and finally analyzed the reconstructed signal using a 1.5-dimensional envelope spectrum [10].

NOPO has several characteristics, including diversity in dissemination, immediate suddenness, crowd fragmentation, and sustained repetition. Many scholars have conducted in-depth studies on OPO management in today's complex network situation. After analyzing the network behavior of online social networks such as Sina Weibo, M. Liu and L. Rong established a dynamic OPO model that takes into account erroneous information and Public Opinion Dissemination (POD). This model introduced the characteristics of online communication, developed multiple dimensions of opinion interaction schemes, and comprehensively considered other public opinion influencing factors. Through simulation experiments, the intervention effects of different official responses were determined [11]. Y. Li and J. Wang constructed a conceptual model grounded on the structural features of a Dual Layer Online Social Network (DLOSN) and designed a cross-network propagation model for OPO. Their propagation characteristics were discussed through numerical simulation. DLOSN had a strong promoting effect on the POD, and intervention should be carried out in the early stages of POD under this model [12]. B. Peng et al. proposed a method for identifying and evaluating online rumors using intuitionistic fuzzy language sets and integration methods. The method first used non-additive measures and integral to calculate the comprehensive evaluation of OPO, and then used generalized functions to determine attribute weights. The example of OPO risk in haze indicated that this method had good performance in identifying and evaluating network rumors, and could be applied to emergency management of OPO [13]. C. Li et al. proposed a new OPO emotion analysis model based on asynchronous networks to analyze the evolution characteristics of OPO emotions in complex environments. Subsequently, using graphic evaluation and review techniques for expansion, a model-based sentiment analysis algorithm was designed. This model extended previous static models and provided a method for extracting viewpoint evolution patterns in complex environments [14]. Y. Dong et al. proposed a public opinion dynamics model for the interaction mechanism between online and offline social networks. The analysis conditions for consensus formation in the public opinion reform model were studied, and the dynamic impact of online agents on public opinion formation was simulated. This model reduced the number of opinion clusters while shortening the steady-state time, and smoothed out the changes in opinion dynamics [15]. Finally, the research areas, indicator testing results, and limitations of the literature review are summarized, as shown in Table 1.

Table 1: Literature summary

Authors	Year	Algorithms/Methods used	Key results	Limitations
B. Muthazhagan et al. [6]	2023	Sooty-LuCaNet	The average classification accuracy of lung cancer detection and classification: 99.16%	Limited to medical image processing
J. Wang et al. [7]	2024	mSTOA	Reduced energy consumption by 35.06%	Specific to mine ventilation systems
H. Jia et al.[8]	2021	STOA-DE	Minimum run time:7.09s Malicious detection accuracy: 99.73%	Limited application in feature selection
J. He et al. [9]	2023	ESTOA	Improved global search	Complexity in

			capability	implementation
J. Zhang et al. [10]	2022	STOA-VMD for fault diagnosis in planetary gearboxes	Effective fault characteristic identification	Limited to fault diagnosis applications
M. Liu and L. Rong [11]	2022	Multi-dimensional opinion dynamic model with misinformation diffusion	Effective intervention simulation	Focused on misinformation diffusion
Y. Li and J. Wang [12]	2022	Cross-network propagation model for public opinion	Promoted early-stage intervention	Specific to dual-layer online social networks
B. Peng et al. [13]	2022	Fuzzy language sets for online rumor identification	High performance in rumor detection	Focused on emergency management
C. Li et al. [14]	2023	Asynchronous network-based sentiment analysis model	Accurate emotion evolution analysis	Limited to sentiment analysis
Y. Dong et al. [15]	2021	Public opinion dynamics model in social networks	Reduced opinion clusters, stabilized dynamics	Older model, may need updates

Combined with Table 1, it is of great significance to manage and control NOPO for college students. Many scholars have studied the STOA and the management of NOPO. Some progresses are made, but most of them focus on the impact analysis of a single factor. Traditional public opinion monitoring methods face challenges such as large data volume and fast information update. In addition, there is a gap in the existing literature in the comprehensive classification and prediction of OPO management, especially in the trend propagation data and the prediction of OPO development trends. The majority of extant studies have not fully addressed the dynamic and multi-faceted nature of college students' OPO. Furthermore, they have not integrated a variety of advanced strategies to improve accuracy and efficiency. Therefore, this study combines STOA with SVM and proposes a public opinion classification algorithm based on STO-SVM. By introducing the Tent Chaos Mapping (TentCM), Adaptive t-Distribution Variation Factor (AtDVF), and Random Walk (RW) strategies into the original STOA, and combining them with Elman Neural Network (ElmanNN), an improved STOA-based NPO influence prediction model, namely ISTOA, is proposed. It aims to improve the efficiency and accuracy of public opinion monitoring and make temporal predictions of the development trend, providing more accurate and efficient solutions for the identification and prediction of NOPO.

2 Methods and materials

This study first combines STOA with SVM and proposes the NOPO classification model, STOA-SVM. Searching for the optimal Penalty Factor (PF) and Kernel Function (KF) of SVM through STOA can improve the convergence speed and accuracy while avoiding overfitting of the model. Secondly, in response to the significant impact of Elman's initial weights, STOA is introduced and improved on the original STOA using TentCM, AtDVF, and RW. An improved ElmanNN NPO prediction model, ISTO-E, is proposed.

2.1 Construction of NOPO recognition and classification model based on improved sooty tern optimization algorithm

Similar to the seagull optimization algorithm, STOA is a biomimetic metaheuristic algorithm developed by scholars such as Gaurav based on industrial engineering, which simulates the migration and hunting behavior of the black tern population. It simulates migration and foraging behavior to solve optimization problems [16]. Compared to traditional optimization methods like ant colony algorithm and Particle Swarm Optimization (PSO), STOA has stronger global search ability, higher solution accuracy, and faster convergence speed. It can provide excellent technical support in type recognition and trend prediction of NOPO [17]. The specific structure of the algorithm is shown in Figure 1.

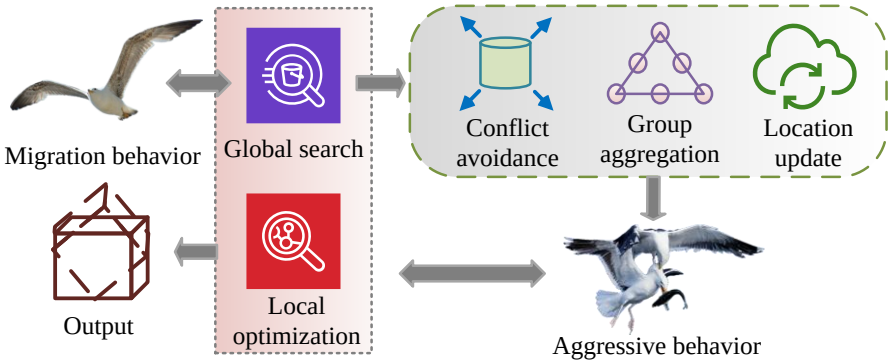

Figure 1: STOA structure diagram

In Figure 1, STOA mainly classifies two parts, namely migration behavior and attack behavior, corresponding to the global search and local optimization stages, respectively. Migration exploration behavior mainly includes three steps: conflict avoidance, group gathering, and location updating. Firstly, in the conflict avoidance step, it is necessary to calculate the position after collision avoidance to avoid collisions with other terns. Secondly, during the migration process, the black tern will approach the optimal position among adjacent black terns, and continuously update its position as it moves towards the optima. While avoiding conflicts, the calculation of the collision avoidance position is equation (1) [18].

$$\begin{cases} c_{st} = S_A \times p_{st} \left| (Z) \right. \\ S_A = C_f - Z(C_f / Z_{\max}) \end{cases} \quad (1)$$

In equation (1), c_{st} represents the movement position of the crow tern after avoiding position collision. S_A represents the new position variable under collision avoidance conditions. p_{st} represents the current location of the black tern. Z refers to the number of iterations. $Z_{\max}$ is the maximum Z. C_f represents a constant used to adjust S_A. Subsequently, the movement of the crow tern towards the optimal solution position is calculated using equation (2).

$$\begin{cases} m_{st} = C_B \times (p_{best}(Z) - p_{st}(Z)) \\ C_B = 0.5 \times R_{and} \end{cases} \quad (2)$$

In equation (2), m_{st} is the process by which the current position p_{st} approaches the optimal position. p_{best} is the optimal solution position. $p_{best}(Z)$ is the optimal location for the tern. C_B is a random variable, which can increase the random factor in the search space. $R_{and} \in [0,1]$ is a random number. The trajectory update calculation towards the optimal solution position is equation (3).

$$d_{st} = c_{st} + m_{st} \quad (3)$$

In equation (3), d_{st} represents the trajectory approaching the optimal solution from the current position. During the migration process, the black tern will continuously adjust its flight speed and attack angle through a spiral hovering method. The expression of its hovering motion in the air is equation (4).

$$\begin{cases} x' = R_{adius} \times \sin(i) \\ y' = R_{adius} \times \cos(i) \\ z' = R_{adius} \times i \\ R_{adius} = u \times e^{kv} \end{cases} \quad (4)$$

In equation (4), x', y', and z' are spatial coordinate values. R_{adius} is the radius of each helix. $i \in [0, 2\pi]$ is the angle variable. e represents the natural logarithmic basis. u and v are the helix angle parameters, set to 1. After calculating the approach to the optimal solution, the iterative formula for the global optimal solution is equation (5).

$$p_{st}(Z) = (d_{st} \times (x' + y' + z')) \times p_{best}(Z) \quad (5)$$

Based on a series of calculations on migration behavior and attack behavior, the implementation process of the STOA is shown in Figure 2.

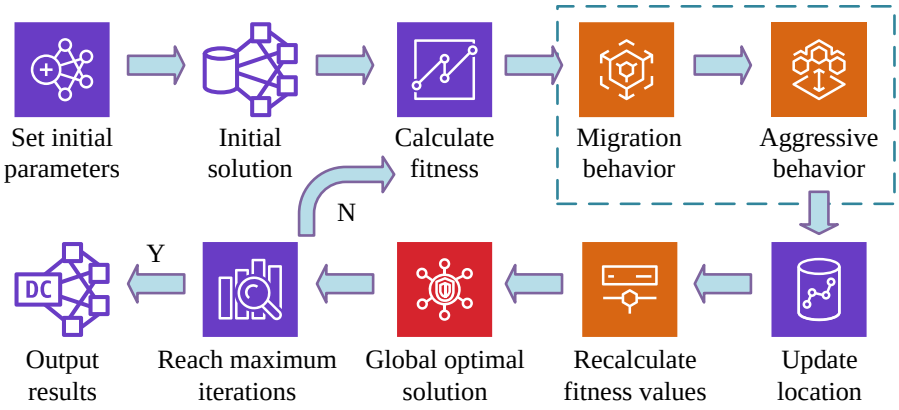

Figure 2: The process of STOA

In Figure 2, the first step is to set the maximum iterations, population size, and other related parameters, and generate several initial solutions. Subsequently, the fitness of each solution is calculated, followed by the migration and attack behavior of the black tern. Then the fitness value based on the new location is recalculated and the global optimum is recorded. Finally, if the current iteration reaches the maximum iterations, run and output the result are stopped. Otherwise, the individual fitness is recalculated. This study selects SVM from numerous machine algorithms that can classify and recognize NOPO, which can be used for numerical prediction and classification tasks of linear and nonlinear data. An STOA-SVM classification algorithm is proposed by combining STOA with SVM. SVM mainly includes Linear Separable-SVM (LS-SVM) and Nonlinear Separable-SVM (NS-SVM), as shown in Figure 3 [19].

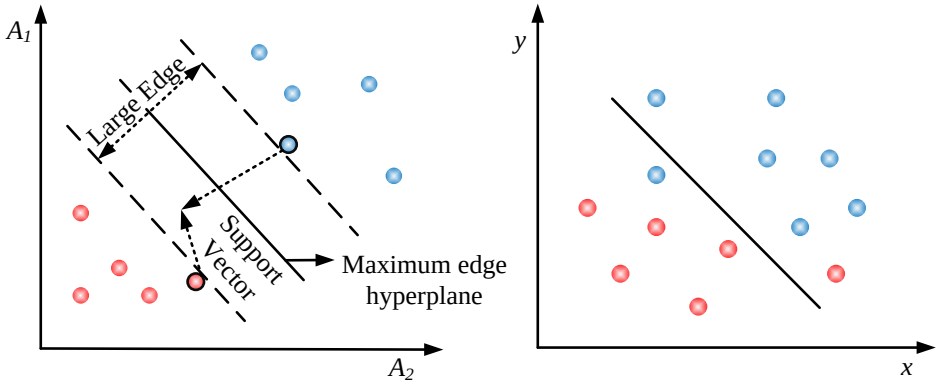

(a) Linear separable support vector machine

(b) Nonlinear separable support vector machine

Figure 3: SVM schematic diagram

Figures 3 (a) and (b) show LS-SVM and NS-SVM, respectively. LS-SVM effectively classifies different samples by searching for the largest edge hyperplane in the feature library space [20-21]. Assuming the existence of dataset D, i.e., $(X_1, y_1), (X_2, y_2), \cdots, (X_{|D|}, y_{|D|})$, where X_i represents the training tuple, y_i represents the class label, and y_i has a value of +1 or -1. The expression of the separation hyperplane is equation (6) [22].

$$w\varphi(x) + b = 0 \tag{6}$$

In equation (6), w is the weight vector, which is the method vector of the hyperplane. b represents a scalar. The PF and KF can directly affect the classification performance of SVM, and the expression of the PF is equation (7) [23].

$$L(\omega, \xi) = \frac{1}{2}\|\omega\|^2 + C(\sum_{i=1}^{l} \xi_i) \tag{7}$$

In equation (7), C represents the PF. Due to the fact that NOPO is a nonlinear data, according to the Lagrange formula, the abstract problem planning expression is equation (8) [24].

$$\begin{cases} \min_{\alpha} \frac{1}{2}\sum_{i=1}^{M}\sum_{j=1}^{M}\alpha_i\alpha_j y_i y_j k(x_i, x_j) - \sum_{i=1}^{M}\alpha_i \\ s.t.\sum_{i=1}^{M} a_i y_i = 0 \end{cases} \tag{8}$$

In equation (8), α_i represents the Lagrange multiplier. From this, the classification decision function

can be obtained, as shown in equation (9) [25].

$$f(x) = sign(\sum_{i=1}^{M} \alpha_i^* y_i \exp(-\frac{\|x - x_i\|^2}{2g^2}) + b^*) \quad (9)$$

In equation (9), g represents the KF parameter. Using STOA to optimize the selection of PF C and KF g can improve the Classification Accuracy (CA) and convergence speed of SVM while avoiding overfitting. Therefore, based on the above calculations, the proposed STO-SVM model flow for identifying NOPO is shown in Figure 4.

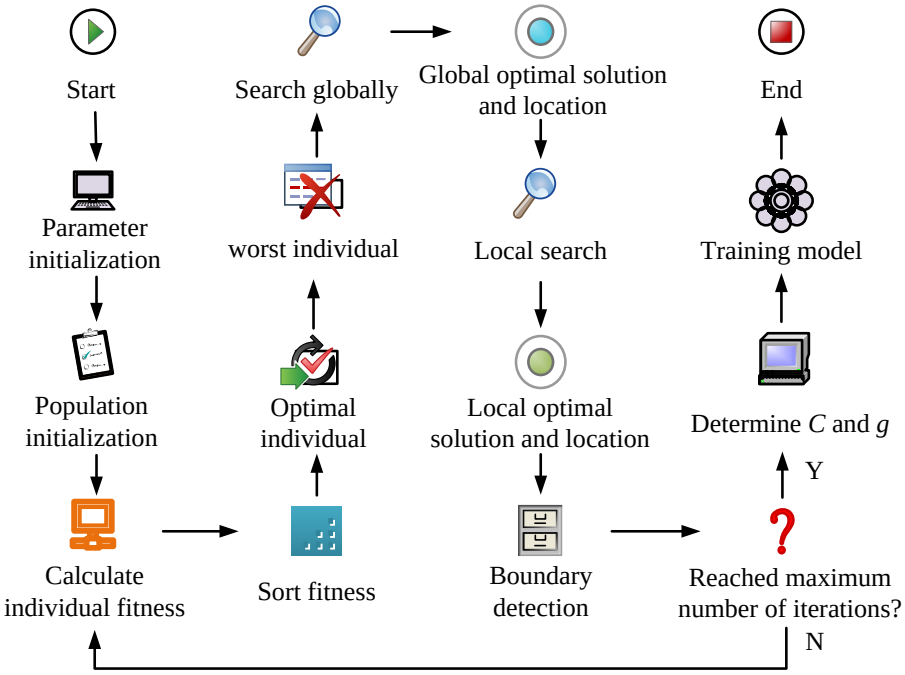

Figure 4: STO-SVM model process

In Figure 4, the first is to initialize the population parameters of the black tern and set the maximum iterations, population size, and parameter optimization boundary. Secondly, the population is initialized to obtain the initialized individuals of the black tern, and their fitness is calculated through SVM. Then, the individuals of the black tern are sorted according to their fitness. The optimal and worst individuals are identified, and the initial optimal solution and position are determined. Subsequently, the black tern is used to search the entire world and obtain the global optimal solution and location. Furthermore, a local search on the population of black terns is conducted to determine the local optimal solution and location. Boundary detection is performed again to search for the position of each individual. Finally, if the maximum iterations is reached at this point, SVM determines the optimal PF C and KF g, outputs the results, trains the model to classify and recognize public opinion, and recalculates the individual fitness of the black tern.

2.2 Construction of elman's OPO prediction model based on improved sooty tern optimization algorithm

After constructing an NOPO classification and recognition model based on STOA, this study attempts to predict the development trend of OPO from the time dimension. Traditional neural networks perform well in handling static data, however, NOPO prediction is a dynamically changing data stream with strong nonlinear characteristics and temporal correlation. To achieve good temporal performance in NOPO prediction, an Elman dynamic feedback neural network is introduced to reflect the dynamic process of the system. ElmanNN is similar to feed-forward neural networks, but has more powerful computing power, with associative memory ability while optimizing computation. Its architecture is shown in Figure 5.

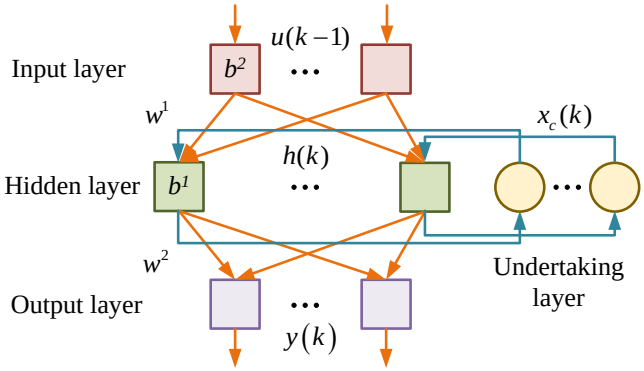

Figure 5: ElmanNN architecture

In Figure 5, ElmanNN mainly contains layers of input, hidden, connection, and output. Compared to back-propagation neural networks, it has an additional layer of connection layer used to form the local feedback part. The transfer function of the connection layer is a linear function. With the increase of delay units, the connection layer can remember past states and use them as inputs to the hidden layer along with the network at the next moment. This feature endows the network with dynamic memory function, stronger sensitivity to historical data, and extremely high applicability to event sequence prediction problems. The model process formula is equation (10).

$$\begin{cases} x_c(k) = \alpha \cdot x_c(k-1) + h(k-1) \\ h(k) = f(w^1 u(k-1) + w^3 x_c(k) + b_n) \\ y(k) = g(w^2 h(k) + b_y) \end{cases} \quad (10)$$

In equation (10), k is the iteration time step. $\alpha \in [0,1]$ is the self-connected feedback gain factor. $x_c(k)$ and $h(k)$ are the output values and quantities of the model's connecting layer and hidden layer at time k. b_n and b_y are the threshold vectors of the hidden and the output layers. $y(k)$ is the output vector at time k. $g(\cdot)$ and $f(\cdot)$ are the activation functions of the output and the hidden layer neurons. $f(\cdot)$ is generally a linear function. $g(\cdot)$ is a nonlinear function. w^1 represents the weight between the output layer and the hidden layer. w^2 is the weight between the layers (hidden/output). w^3 represents the weight between the hidden layer and the receiving layer. The feed-forward connection block composed of input, hidden, and output layers can adjust its weight, that is, w^1 and w^2 can be updated through correction. However, the recursive part composed of the hidden and the connecting layers cannot be corrected by weight, that is, the w^3 value is fixed. Traditional ElmanNN usually uses gradient descent back-propagation algorithm for training, following error correction learning rules. The input layer inputs data to the hidden for processing, and then the output layer propagates the results forward for the input signal [26]. When the error between the actual output of the output layer and the expected output is large, error back-propagation is adopted, which means that the error signal is back-propagated to the neurons in each layer. By using such methods, the weights and threshold matrices of neurons are updated and corrected [27]. The training error function of ElmanNN is equation (11) [28].

$$E(W)(k) = \frac{1}{2}(\bar{y}(k) - y(k))^T (\bar{y}(k) - y(k)) \quad (11)$$

In equation (11), $y(k)$ represents the actual value output at step k during the training process. $\bar{y}(k)$ is the expected output value. Finding the appropriate W^* and $E(W^*) = \min E(W)$ is achieved through continuous iterative calculations. Finding the weight matrix that minimizes the objective function value is the purpose of network learning [29]. The formula for updating the weight matrix is equation (12) [30].

$$\begin{cases} W = W + \Delta W \\ \Delta W = -\eta \dfrac{\partial E}{\partial W} \end{cases} \quad (12)$$

In equation (12), W represents the error function and η represents the learning rate. By searching for the minimum matrix, error correction learning can be transformed into a classic optimization problem. However, in practical applications, Elman has the drawback of having a significant initial weight impact and being prone to falling into local optima. Therefore, this study also introduces STOA and improves the original STOA by using three strategies: TentCM, AtDVF, and RW, to improve its computational time and later search convergence efficiency. Firstly, the TentCM is used to enhance population diversity in the initial stage of the algorithm. It replaces the originally randomly generated individuals with individuals initialized by chaotic mapping, which can effectively increase the diversity and diffusion of the initial population. The TentCM function is equation (13).

$$z_{k+1} = \begin{cases} 2z_k, & 0 \le z_k \le 0.5 \\ 2(1-z_k), & 0.5 \le z_k \le 1 \end{cases} \quad (13)$$

In equation (13), $k = 0,1,2,...$ represents 1 mapping degree. z_k represents the function value of the k-th

mapping. Replacing the original randomly generated individuals of the black tern with those initialized by TentCM can effectively increase the population diversity. This mapping function can ensure that the initial population points are more evenly distributed, prevent premature convergence, and enhance global search capabilities. Subsequently, AtDVF is introduced during the global search phase of individuals, which can effectively break out of local optima and solve for new fitness values. The AtDVF adjusts the search strategy according to the population distribution to ensure a balance between exploration and exploitation. Its probability density function expression is shown in equation (14).

$$P_t(x) = \frac{\Gamma(n+1/2)}{\sqrt{n\pi}\cdot\Gamma(n/2)}\cdot(1+\frac{x^2}{n})^{-\frac{n+1}{2}} \quad (14)$$

In equation (14), Γ represents the gamma function. n represents the degree of freedom. x represents the random variable, and $P_t(x)$ represents the probability function value of the random variable under the t-distribution with n degrees of freedom. Finally, the optimal solution random walk strategy further enhances the optimization process by introducing random motion in the search space. This strategy updates the position of the optimal value and generates a new position after the individual searches for the local optimal value. Its expression is shown in equation (15).

$$X(t) = [0, cussum(2r(t_1)-1), .., cussum(2r(t_n)-1)] \quad (15)$$

In equation (15), t represents the step size of individual RW. $cussum$ is the total sum of individuals during their wandering process. $X(t)$ represents the set of steps. This strategy updates the position of the optimal value and generates a new position after the individual searches for the local optimal value, compares it with the current optimal solution, and replaces it if it is better. This strategy allows individuals to perform random walks, which helps to escape from local optima and ensure a robust search process. ISTOA is used to optimize ElmanNN, and an NOPO prediction model based on ISTO-E is proposed. The process is shown in Figure 6.

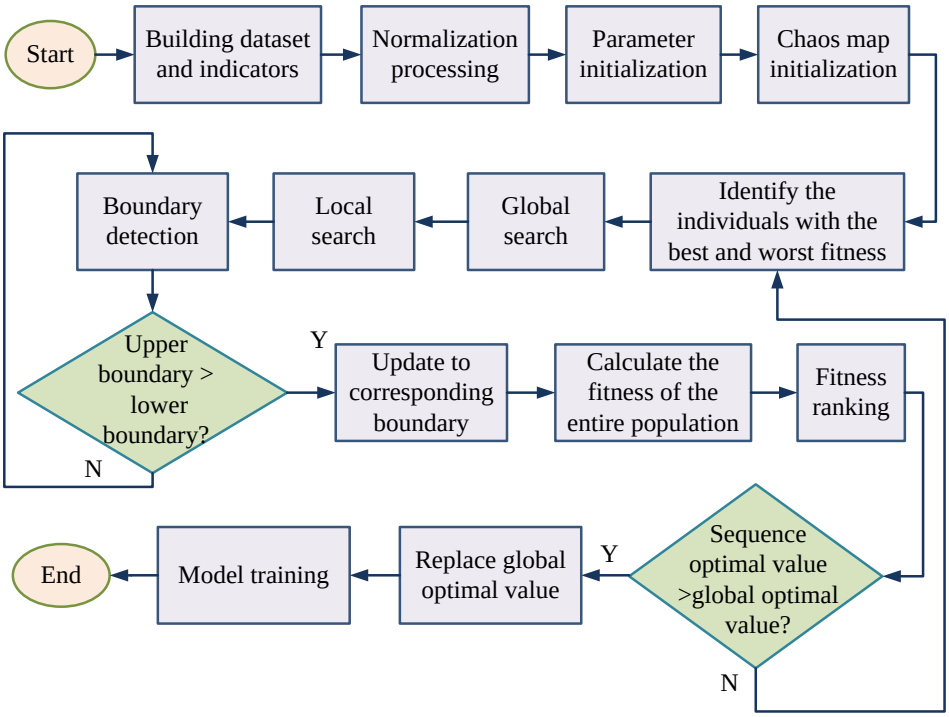

Figure 6: ISTO-E model process

In Figure 6, the first step is to construct the original dataset and then construct the corresponding NOPO impact prediction indicator set based on the dataset. Secondly, the data is normalized and the population parameters of the black tern are initialized, with the maximum iterations, population size and parameter optimization boundaries, and adjustable parameters set. Subsequently, the population is initialized through chaotic mapping, and the fitness of the initialized individuals is calculated and sorted. The next step is to identify the individuals with the best and worst fitness, determine the initial optimal solution and its position, and then conduct a global search to obtain the global optimum and its position. Further local search of the population is conducted to determine the local optimum and location. The upper and lower boundaries obtained from boundary detection are compared, and if they are greater than, they are updated to the corresponding boundaries. Then, the

fitness of the entire population is calculated and ranked. If the optima in the sequence surpasses the global optima, it is replaced. Otherwise, iteration continues until Elman's optimal weight threshold parameter is obtained. Finally, Elman uses the optimal value, which is the optimal weight threshold parameter, to train and obtain the prediction model.

3 Results

To verify the effectiveness of improving the NOPO classification and prediction model, this study first establishes a suitable experimental environment and cleans and preprocesses the experimental data. Part of the data is utilized for model training, while the other part is used for testing different indicators of model performance. The first section tests the performance of the STO-SVM classification method, while the second section conducts experiments on the NOPO trend prediction performance of ISTO-E. All models in the experiment use the same dataset and parameters to ensure the accuracy of the experiment.

3.1 Performance testing of STO-SVM public opinion classification model

To test the performance of the STO-SVM in NOPO classification, this study used a Windows 10 system with an Intel (R) CPU of Intel Core i7 and 16GB of memory, and the experimental software was Matlab. SVM, PSO-SVM, and STO-SVM were introduced for comparative testing. The experiment adopted the commonly used UCI machine learning standard test dataset, which includes 148 datasets with different instances, features, and categories. The first step was to test the CA of the three algorithms on different datasets, which covers different fields including medical diagnosis, image recognition, text classification, etc. The study selected libras_movement, balance, blood, and mean datasets, and deleted missing or inconsistent data entries to ensure the integrity of the dataset. Then the feature values were scaled to a standard range to prevent larger range features from dominating the learning process. Finally, relevant features were identified and retained to reduce dimensionality and improve model performance. The study set the optimal penalty factor C to 494.36 and the kernel function g to 10.95, the step size is set to 0.5. The population size was set to 40, with 100 iterations. Ten experiments were conducted on each dataset, and the results are shown in Figure 7.

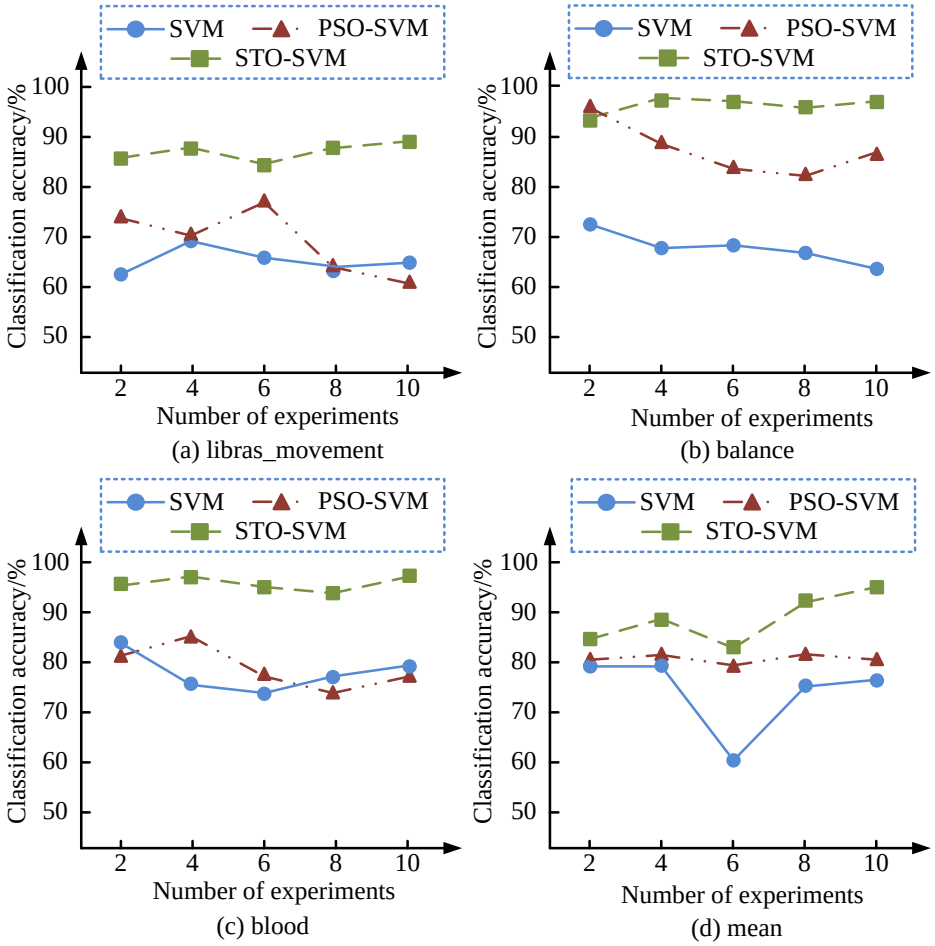

Figure 7: Comparison of CA of classifiers

Figures 7 (a) to (d) show the CA test results of three classifiers on the libras_movement, balance, blood, and mean datasets, respectively. In Figure 7 (a), STO-SVM has the highest CA with all above 80% and has the highest stability. The average CA of SVM and PSO-SVM are 64.58% and 69.75%, respectively. In Figure 7 (b), the 10 tests of STO-SVM all show a CA of over 90%, with the optimal CA. The average CA of SVM and PSO-SVM are 68.86% and 70.24%, respectively. In Figure 7 (c), the CA of STO-SVM is significantly better than other comparison models, with an average CA of 77.83%, 79.80%, and 95.87%. The accuracy of PSO-SVM is slightly higher than the SVM. In Figure 7 (d), the average CA of SVM, PSO-SVM, and STO-SVM classifiers on the dataset blood are 75.84%, 80.39%, and 89.57%, respectively. The CA of PSO-SVM is the most stable in ten experiments, fluctuating around 80%. To reflect the variability of CA of different models, the 95% Confidence Interval (CI) of each indicator is calculated. Table 2 shows the CA of each model on different data sets and its 95% CI.

Table 2: Confidence level calculation results

Dataset	CA of SVM (%)	CA of PSO-SVM (%)	CA of STO-SVM (%)
Libras_movement	64.58 ± 2.14	69.75 ± 1.87	80.23 ± 1.23
Balance	68.86 ± 2.31	70.24 ± 2.12	91.15 ± 1.05
Blood	75.84 ± 1.89	80.39 ± 1.76	89.57 ± 0.98
Mean	77.83 ± 1.54	79.80 ± 1.42	95.87 ± 0.85

Table 2 shows the calculation results of the 95% CI of the three classifiers, SVM, PSO-SVM, and STO-SVM, on different data sets. The CI provides information about the variability of the performance of each classifier. On the libras_movement data set, the CA of STO-SVM is 80.23%, and its 95% CI is ±1.23. This means that the 95% CI of STO-SVM on this dataset ranges from 79.00% to 81.46% CA. Secondly, the Precision-Recall (PR) curves of the three classifiers on the same dataset are shown in Figure 8.

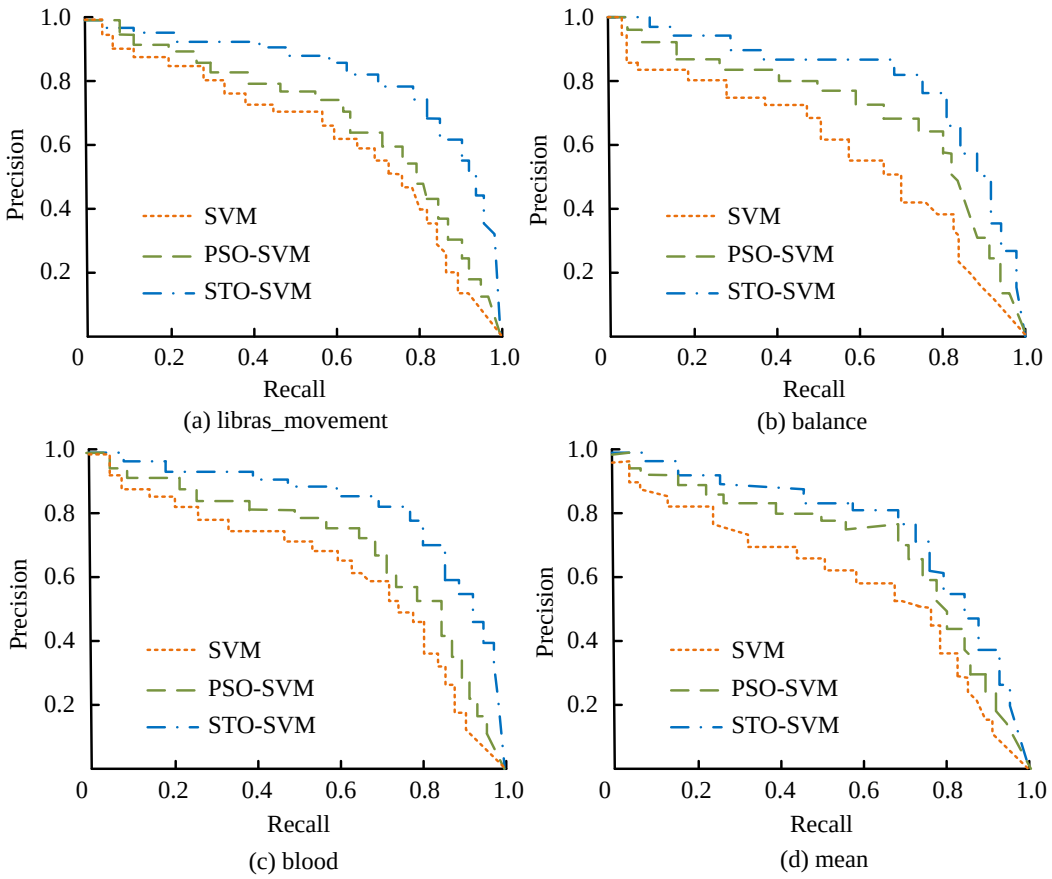

Figure 8: Comparison of classifiers PR curves

Figures 8 (a) to 8 (d) show the PR curves of three classifiers on the libras_movement, balance, blood, and mean datasets, respectively. The PR curve is a commonly used graphical tool in machine learning to evaluate the

performance of binary classification models, which can intuitively reflect the performance of classifiers. If the curve of a classifier completely surrounds the curves of other classifiers, it indicates that the classifier performance is better. In Figure 8, the STO-SVM curve completely envelops the PR curves of SVM and PSO-SVM in all datasets, while the PSO-SVM curve completely envelops the SVM curve. This proves that the performance of STO-SVM is the best among compared classifiers, while the PSO-SVM is lower than STO-SVM and better than traditional SVM. Therefore, STO-SVM has good CA and performance. Subsequently, the study uses web crawler data to crawl OPO data from Sina Weibo. The dataset includes posts and comments related to various public opinion topics from June 2022 to January 2023. The dataset contains approximately 100,000 entries, each of which includes text content, timestamp, user information, and related public opinion categories, such as current affairs, economy, culture, and society. At the same time, the study preprocesses the data to eliminate noise and irrelevant information, such as advertisements and spam. Three text normalization techniques, tokenization, stop word removal, and stem extraction, are applied to preprocess the data for subsequent analysis. The top 100 OPO events are selected as the test dataset, with a ratio of 8:2 between NPO and non-NPO events. Table 3 shows the multi-indicator test data for four models.

Table 3: Metrics test results for different algorithms

Index	Algorithm		
	SVM	PSO-SVM	STO-SVM
P/%	68.48	84.57	92.86
R/%	64.82	68.91	93.75
F1/%	55.97	75.83	93.82
Resource consumption rate/%	21.58	37.66	18.63
Average detection time/s	9.3	14.5	9.1

In Table 3, the classification model based on STO-SVM algorithm achieves test results of 92.86%, 93.75%, and 93.82% in accuracy, recall, and F1 values for 100 public opinion events, respectively, which are superior to other comparative models. In terms of resource consumption rate, STO-SVM is 18.63%, which is lower than a single SVM model. The resource consumption rate of PSO-SVM is 37.66%, which is the highest among all models. In terms of model computation time, the average time of SVM, PSO-SVM, and STO-SVM classifiers is 9.3s, 14.5s, and 9.1s, respectively. PSO-SVM takes the longest running time, followed by SVM, slightly higher than STO-SVM. Therefore, STO-SVM has significant comprehensive advantages compared to comparative models. Similarly, to analyze the resource consumption and average detection time of each model in detail, the confidence intervals of each model are shown in Table 4.

Table 4: Confidence level calculation results

Index	SVM	PSO-SVM	STO-SVM
P/%	68.48±2.13	84.57±1.85	92.86±0.95
R/%	64.82±2.08	68.91±2.01	93.75±0.88
F1/%	55.97±1.93	75.83±1.78	93.82±0.92
Resource consumption rate/%	21.58±0.85	37.66±1.23	18.63±0.65
Average detection time/s	9.3±0.2	14.5±0.3	9.1±0.1

Table 4 shows the CI calculation results of each model under different indicators. The resource consumption rate indicates the computing resource occupancy rate required by the model for classification. The table shows that the STO-SVM can effectively reduce the use of computing resources when processing large amounts of data. The CI of the resource consumption rate of ±0.65 further illustrates the consistency and reliability of STO-SVM in multiple experiments. The average detection time refers to the average time required for the model to complete the classification task. The fast detection time of STO-SVM can be attributed to its optimized global and local search strategies, which make it more efficient when processing large-scale data. The CI of the detection time of ±0.1 also shows the stability of STO-SVM in different tests. Finally, to verify the model feasibility in classifying public opinion types, this study set up three models to test the recognition accuracy of four different public opinion topics: current politics, economy, culture, and social public opinion, as shown in Figure 9.

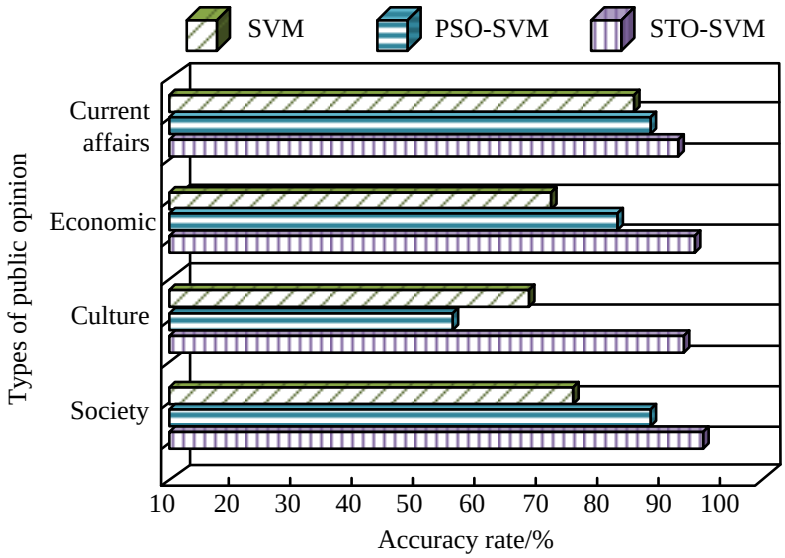

Figure 9: CA for different public opinion topics

Figure 9 shows the CA of three models for current affairs, economy, culture, and social public opinion categories. Among the four different OPO categories, STO-SVM has the best CA. In the classification of current political public opinion, the CA of SVM, PSO-SVM, and STO-SVM are 88.62%, 90.87%, and 94.33%. In the classification of economic public opinion, STO-SVM holds the best accuracy, with SVM and PSO-SVM having CAs of 73.51% and 83.57%. In cultural public opinion, SVM's CA is superior to PSO-SVM, and the STO-SVM model still holds the optimal accuracy. In terms of social opinion classification, the CA of SVM, PSO-SVM, and STO-SVM are 78.34%, 90.04%, and 98.98%. In summary, STO-SVM has stronger OPO recognition and classification capabilities, and excellent computational efficiency, which can achieve more efficient OPO detection.

3.2 Comparison experiment of ISTO-E public opinion trend prediction model

This study further conducts experimental testing on ElmanNN based on ISTOA, with the same experimental environment as the previous section. To verify the performance of ISTOA, nonlinear unimodal and nonlinear multi-modal functions are first selected as benchmark test functions to test the convergence and global optimization capabilities. The specific information of the functions is listed in Table 5.

Table 5: Detailed information of test functions

Function		Formula	Parameter range	Dimension
Unimodal function	F_1	$f_1(x)=\sum_{i=1}^{n-1}\left[100(x_{i+1}-x_i^2)^2+(x_i-1)^2\right]$	$[-100,100]$	30
	F_2	$f_2(x)=\sum_{i=1}^{n}x_i^2$	$[-100,100]$	30
Multi-modal function	F_3	$f_3(x)=\sum_{i=1}^{n}\left[x_i^2-10\cos(2\pi x_i)+10\right]$	$[-5.12,5.12]$	30
	F_4	$f_4(x)=\sum_{i=1}^{N}\frac{x_i^2}{4000}-\prod_{i=1}^{N}\cos(\frac{x_i}{\sqrt{i}})+1$	$[-600,600]$	30

In Table 5, the selected unimodal functions are F_1 and F_2, which can evaluate the algorithm's development ability, i.e. convergence performance. The multi-modal test functions are F_3 and F_4, which can evaluate whether the algorithm has the ability to jump out of local optimum, that is, the global optimization ability. In the experiment, the dimensions of each function are 30, the population is 30, and the maximum iteration is 500. PSO, Whale Optimization Algorithm (WOA), and ISTOA are selected for comparative testing, as shown in Figure 10.

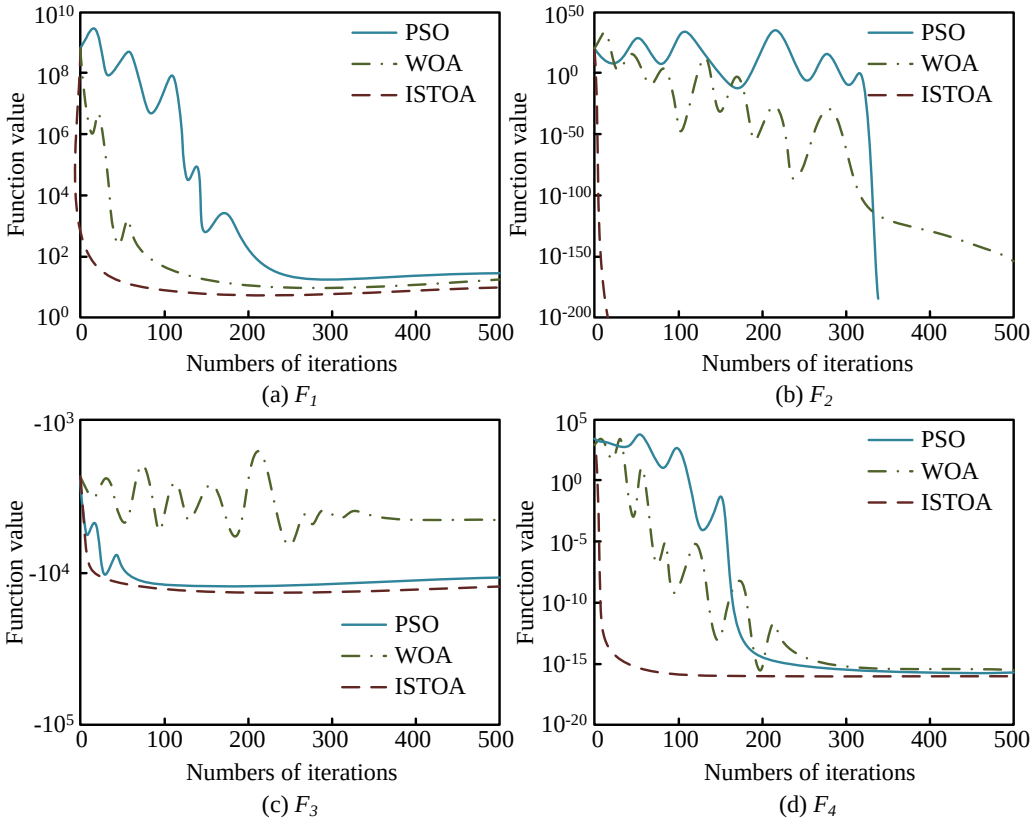

Figure 10: Comparison of algorithm convergence curves

Figures 10 (a) to 10 (d) are the convergence curves of three algorithms on four standard test functions F_1, F_2, F_3, and F_4. On the unimodal functions in Figures 10 (a) and 10 (b), ISTOA quickly converges to find the global minimum and the curve oscillates less. PSO and WOA algorithms exhibit slow convergence speed and large curve oscillations. The convergence speed of WOA algorithm is slightly better than PSO, but there is a gap compared to ISTOA. On the multi-modal functions in Figures 10 (c) and 10 (d), ISTOA also shows a fast convergence trend, with a better convergence curve than PSO and WOA. WOA exhibits maximum oscillation in the early stage of convergence on multi-modal functions, and reaches convergence state after 364 and 298 iterations on F_3 and F_4 functions. The PSO curve oscillates less and reaches convergence after 92 and 284 iterations on the F_3 and F_4 functions. In summary, ISTOA has excellent convergence speed and accuracy, with significant improvements in both global search and local exploration. On the basis of verifying the good performance of ISTOA, this study further verifies the performance of the ElmanNN NPO prediction algorithm based on ISTOA. This study introduces traditional Elman, Output-Input Feedback Elman (OIF-Elman), and ISTO-E neural networks for comparative experiments. The OPO event dataset is used, and the error results of the three models repeating 500 simulation experiments on the dataset are listed in Table 6.

Table 6: Average prediction experiment values for different models

Error target	Model	Training frequency	Training error	RMSE	MSE	MAPE	Success rate
Error<0.5	Elman	68	1.0215	0.8574	0.1458	4.57	42.90
	OIF-Elman	57	0.8564	0.8354	0.1136	3.39	49.68
	ISTO-E	49	0.1853	0.6054	0.0876	1.77	86.95
Error<0.1	Elman	128	0.1458	1.2586	0.1477	6.58	22.98
	OIF-Elman	119	0.0849	1.0239	0.0823	5.87	29.34
	ISTO-E	94	0.0725	0.852	0.0687	2.21	37.85

Table 6 shows the average results obtained by three models on the public opinion event dataset after 500 repeated experiments. The smaller the values of Root Mean Square Error (RMSE), Mean Square Error (MSE), and Mean Absolute Percentage Error (MAPE), the better the predictive performance and the closer the predicted values match the true values. When the error target is less than 0.5, the success rates of Elman, OIF-Elman, and ISTO-E are 42.90%, 49.68%, and 86.95%, respectively. The ISTO-E model has the best average error value and requires the least average number of times for model training. When the error target is less than 0.1, the error values of the three models increase to different degrees. The RMSE, MSE, and MAPE values of the ISTO-E model are the smallest among the comparison models, and the success rate is the best. Subsequently, a certain public opinion event is extracted from the 100 OPO event datasets used in the previous section and tested for practical prediction applications. The test results are displayed in Figure 11.

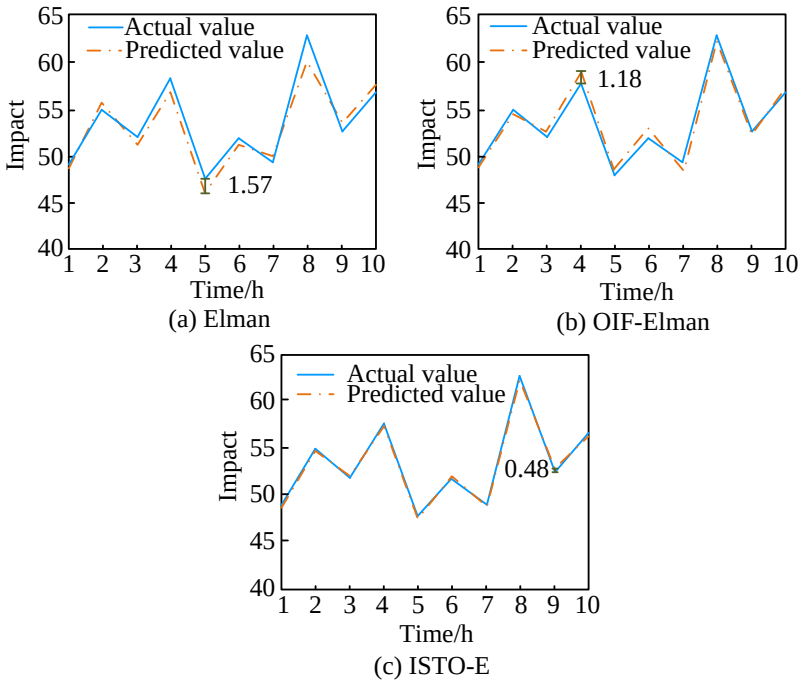

Figure 11: Prediction of public opinion influence over time

Figures 11 (a) to (c) show the predicted and actual impact of public opinion predicted by the Elman, OIF-Elman, and ISTO-E models 10 hours after a certain public opinion event occurs. Figure 11 is that the predicted curve of the ISTO-E is closest to the actual influence value, indicating that the actual difference between the predicted and actual values is small. The Elman model has the lowest fit between the the two value curves, resulting in poor predictive performance. The difference between the two values of the OIF-Elman model is between the two, and the prediction effect is average. The maximum prediction error values of Elman, OIF-Elman, and ISTO-E models are 1.57, 1.18, and 0.48. Finally, 15 events from the public opinion event set are randomly selected, and the impact of the events is predicted 5 hours after their occurrence. Table 7 shows the relevant results.

Table 7: Prediction results of public opinion events

Sample	Actual value of influence	Predicted value			Error value		
		Elman	OIF-Elman	ISTO-E	Elman	OIF-Elman	ISTO-E
1	63.2	63.84	63.42	63.24	0.64	0.22	0.04
2	65.8	66.31	66.42	65.82	0.51	0.62	0.02
3	72.9	71.47	71.98	72.87	-1.43	-0.92	-0.03
4	48.1	48.73	49.82	48.53	0.63	1.72	0.43
5	57.4	58.50	58.22	57.51	1.10	0.82	0.11
6	58.9	60.34	59.87	59.03	1.44	0.97	0.13
7	76.8	74.25	75.33	76.48	-2.55	-1.47	-0.32
8	72.1	71.26	72.07	72.09	-0.84	-0.03	-0.01
9	62.0	62.78	62.34	62.21	0.78	0.34	0.21
10	59.7	60.54	60.28	60.01	0.84	0.58	0.31
11	55.5	53.97	55.58	55.46	-1.53	0.08	-0.04
12	49.3	50.36	51.58	49.77	1.06	2.28	0.47
13	78.4	78.08	78.04	78.05	-0.32	-0.36	-0.35
14	58.2	59.88	59.84	58.46	1.68	1.64	0.26
15	66.4	65.33	65.52	66.38	-1.07	-0.88	-0.02

Table 7 shows the true values of public opinion influence and the predicted values and prediction errors of the three models within the 5th hour after 15 public opinion events occurred. Among all events, the ISTO-E model has the smallest prediction error value, the best prediction accuracy among the three models, and the prediction error value in the eighth public opinion event is only 0.01. The single Elman model has the highest prediction error in most events, which is higher than the other improved OIF-Elman and ISTO-E models. Therefore, the ISTO-E prediction model has better prediction accuracy and better monitoring value in practical applications.

4 Discussion

The current NOPO monitoring and prediction system for college students faces difficulties in extracting numerical features in complex network environments, and the time dimension design of numerical analysis systems is not comprehensive. This study focused on the dissemination trends and values of public opinion events on social media such as the internet. By combining STOA with SVM, an NOPO recognition model based on the STO-SVM fusion model was proposed. At the same time, taking into account the periodicity of POD, STOA has been improved from three aspects. Combined with the ElmanNN model, an ISTO-E neural network model for predicting the trend of public opinion influence has been proposed. In the testing of the STO-SVM public opinion classification model, the CA of STO-SVM reached 95.87%, significantly better than the accuracy (84.57%) of the PSO-SVM model proposed by J. Wang et al. [7] for optimizing energy consumption in MV systems. In addition, the STO-SVM model also showed significant advantages in resource consumption rate and average detection time, with a resource consumption rate of 18.63% and an average detection time of 9.1 seconds. The resource consumption rate of the PSO-SVM was 37.66%, and the mean detection time was 14.5s. This was because the PSO-SVM introduced uniform reverse strategy, fitness distance balance selection strategy, and mutation strategy, and its complex structure might lead to a decrease in computational efficiency in large-scale datasets. Relatively speaking, the STO-SVM model maintained high accuracy while achieving higher computational efficiency, demonstrating better practicality. In the tests of current affairs, economy, culture, and social public opinion, the CA of STO-SVM were 94.33%, 95.83%, 95.06%, and 98.98%, respectively. This was because introducing STOA in a single SVM to search for the optimal PF and KF could effectively improve the convergence speed and accuracy of SVM.

In the performance testing of the ISTO-E prediction model, the improved ISTOA showed a rapid convergence trend on unimodal and multi-modal test functions, demonstrating excellent global and local search capabilities. Its performance was also better than algorithms in other literature. In the improved STOA proposed by J. He et al. [9], although the model performed well in local and global searches, the prediction error in practical applications was still slightly higher than the ISTO-E model in this study. This was because the study introduced the theory of POD trends in the ISTO-E model, which could ensure high predictive accuracy and actual response speed over time. In the testing of 15 public opinion events, the ISTO-E had the smallest prediction error value, the best prediction accuracy among the three models, and the prediction error value in Public Opinion Event 8 was only 0.01. These results show that the STO-SVM model can more efficiently utilize computing resources when processing large-scale data and can provide fast responses in real-time applications. This has important practical significance for application scenarios that require fast processing and real-time analysis, such as social media public opinion monitoring and real-time data analysis. In comparison with existing studies, the research method demonstrates significant advantages. For example, in the

SVM models based on PSO and genetic algorithm commonly used in the literature, there are usually certain limitations in CA and optimization efficiency. The STO-SVM model proposed in this study effectively solves these problems and significantly improves the performance of the model by introducing a variety of optimization strategies. In addition, compared with the traditional SVM model, STO-SVM shows stronger robustness and stability when processing complex data sets and large-scale data, which further verifies the effectiveness and practicability of this research method.

In summary, this study proposes an efficient and accurate NOPO classification and prediction system by combining STOA with SVM, ISTOA with ElmanNN. Research results show that the improved model is superior to existing traditional methods in many aspects, especially in terms of classification accuracy, resource utilization, and time efficiency. This not only provides new ideas and technical means for future public opinion detection and prediction of college students, but also has a positive impact on promoting the healthy and civilized development of the internet. Although the STO-SVM and ISTO-E models proposed in the study perform well in many aspects, they still have some limitations. Although the introduced TentCM, AtDVF and RW strategies have significantly improved the optimization effect, these improvements may still have limitations in some specific scenarios. For example, model performance may be limited for certain highly complex and nonlinear data sets. Furthermore, while the STO-SVM demonstrates efficacy in terms of resource utilization and time efficiency, the practical deployment and application of the model may still encounter obstacles when computing resources are severely constrained.

5 Conclusion

To improve the monitoring effect of NPO among college students, this study combined the STOA and SVM, ISTOA and ElmanNN to build a classification STO-SVM and prediction model ISTO-E for NOPO. The results indicated that the model significantly improved the classification and prediction performance of NOPO. In the experiment, the STO-SVM model showed the best convergence speed and accuracy in different test datasets, and demonstrated the best performance in PR curve, CA, Recall, and F1 value. Simultaneously, it held the highest CA in the classification of four different categories of public opinion. In the ISTO-E prediction model experiment, ISTOA showed good convergence performance on unimodal and multi-modal test functions. In practical applications, the ISTO-E model required lower average training times, errors, RMSE, MSE, and MAPE than the comparison model. In the time series testing of public opinion events, the error between the predicted impact value and the true value was minimized, achieving the optimal prediction effect. Finally, through comprehensive experimental investigation, the superior performance of the STO-SVM and ISTO-E models in multiple indicators was substantiated, and the advantages of these models in terms of resource consumption and time efficiency were elucidated. It offers a valuable point of reference for subsequent research and demonstrates that the STO-SVM and ISTO-E models have significant potential for practical applications. According to the limitations observed in the study, subsequent research can further investigate and improve the STOA in quantum mechanics in the STO-SVM model, and conduct further experiments on the model in conjunction with large-scale computing equipment. In addition, future research can focus on introducing more complex and diverse features, such as semantic analysis, sentiment analysis, and network analysis, to improve the model's ability to detect and predict subtle trends in public opinion. Finally, research can enhance the interpretability of the model by developing visualization tools and user-friendly interfaces, particularly for non-expert users. This will facilitate broader adoption and comprehension of classification and prediction outcomes.

References

[1] P. P. Groumpos, "A critical historic overview of artificial intelligence: issues, challenges, opportunities, and threats," Artificial Intelligence and Applications, vol. 1, no. 4, pp. 197-213, 2023. https://doi.org/10.47852/bonviewAIA3202689

[2] J. Xiong, G. A. Jacob, and J. G. Xiong, "Risk management of negative online public opinion in a tertiary hospital based on the kaiser model," American Journal of Health Behavior, vol. 47, no. 1, pp. 165-172, 2023. https://doi.org/10.5993/AJHB.47.1.17

[3] J. Wang, and Y. Li, "Research on the propagation and governance of public opinion information under the joint action of internal and external factors," Aslib Journal of Information Management, vol. 75, no. 2, pp. 193-214, 2023. https://doi.org/10.1108/AJIM-02-2022-0065

[4] H. Lyu, Y. Fan, Z. Xiong, M. Komisarchik, and J. Luo, "Understanding public opinion toward the StopAsianHate movement and the relation with racially motivated hate crimes in the US," IEEE Transactions on Computational Social Systems, vol. 10, no. 1, pp. 335-346, 2021. https://doi.org/10.1109/TCSS.2021.3136858

[5] C. Liu, and Y. Han, "User information collection of weibo network public opinion under python," Journal of Information Processing Systems, vol. 19, no. 3, pp. 310-322, 2023. https://doi.org/10.3745/JIPS.03.0185

[6] B. Muthazhagan, T. Ravi, and D. Rajingirinath, "Sooty-LuCaNet: Sooty tern optimization based deep learning network for lung cancer detection," Journal of Intelligent & Fuzzy Systems, vol. 45, no. 5, pp. 8823-8836, 2023.

https://doi.org/10.3233/JIFS-232875

[7] J. Wang, Y. Xue, L. Wen, and D. Shi, "Optimization of airflow distribution in mine ventilation networks using the modified sooty tern optimization algorithm," Mining, Metallurgy & Exploration, vol. 41, no. 1, pp. 239-257, 2024. https://doi.org/10.1007/s42461-023-00895-y

[8] H. Jia, Y. Li, K. Sun, N. Cao, and H. M. Zhou, "Hybrid sooty tern optimization and differential evolution for feature selection," Computer Systems Science & Engineering, vol. 39, no. 3, pp. 321-335, 2021. https://doi.org/10.32604/csse.2021.017536.

[9] J. He, Z. Peng, D. Cui, J. Qiu, Q. Li, and H. Zhang, "Enhanced sooty tern optimization algorithm using multiple search guidance strategies and multiple position update modes for solving optimization problems," Applied Intelligence, vol. 53, no. 6, pp. 6763-6799, 2023. https://doi.org/10.1007/s10489-022-03635-9

[10] J. Zhang, Z. Jiang, G. Wu, and H. Bi, "Study on wear fault diagnosis of planetary gearbox based on STOA-VMD combined with 1.5-dimensional envelope spectrum," International conference on the Efficiency and Performance Engineering Network, vol. 8, no. 18, pp. 90-102, 2022. https://doi.org/10.1007/978-3-031-26193-0_9

[11] M. Liu, and L. Rong, "An online multi-dimensional opinion dynamic model with misinformation diffusion in emergency events," Journal of Information Science, vol. 48, no. 5, pp. 640-659, 2022. https://doi.org/10.1177/0165551520977430

[12] Y. Li, and J. Wang, "Cross-network propagation model of public opinion information and its control in coupled double-layer online social networks," Aslib Journal of Information Management., vol. 74, no. 2, pp. 354-376, 2022. https://doi.org/10.1108/AJIM-04-2021-0126

[13] B. Peng, C. Zheng, G. Wei, X. Zhao, and A. Wan, "Risk assessment method on haze networks public opinion based on intuitionistic fuzzy choquet integral," International Journal of Fuzzy Systems, vol. 24, no. 6, pp. 2858-2872, 2022. https://doi.org/10.1007/s40815-022-01300-4

[14] C. Li, Y. Qu, and X. Zhu, "Asynchronous network-based model and algorithm for sentiment analysis of online public opinions," Kybernetes, vol. 52, no. 10, pp. 4130-4157, 2023. https://doi.org/10.1108/K-02-2021-0159

[15] Y. Dong, Z. Ding, F. Chiclana, and E. Herrera-Viedma, "Dynamics of public opinions in an online and offline social network," IEEE Transactions on Big Data, vol. 7, no. 4, pp. 610-618, 2017. https://doi.org/10.1109/TBDATA.2017.2676810

[16] K. Z. Zamli, M. A. Kader, S. Azad, and B. S. Ahmed, "Hybrid henry gas solubility optimization algorithm with dynamic cluster-to-algorithm mapping," Neural Computing and Applications, vol. 33, no. 14, pp. 8389-8416, 2021. https://doi.org/10.1007/s00521-020-05594-z

[17] B. R. Joseph, I. J. Jebadurai, G. J. Paulraj, J. Jebadurai, and M. M. Varuvel, "DEEP VEIN NET: Deep vein thrombosis identification via sooty tern optimized deep learning network," Revue Roumaine des Sciences Techniques, vol. 69, no. 1, pp. 115-120, 2024. https://doi.org/10.59277/RRST-EE.2024.1.20

[18] B. Chitra and S. S. Kumar, "Early cervical cancer diagnosis using sooty tern-optimized CNN-LSTM classifier," International Journal of Imaging Systems and Technology, vol. 32, no. 6, pp. 1846-1860, 2022. https://doi.org/10.1002/ima.22764

[19] S. Saha, A. Saha, T. K. Hembram, B. Kundu, and R. Sarkar, "Novel ensemble of deep learning neural network and support vector machine for landslide susceptibility mapping in tehri region, garhwal himalaya," Geocarto International, vol. 37, no. 27, pp. 17018-17043, 2022. https://doi.org/10.1080/10106049.2022.2120638

[20] Y. B. Zhang, P. Y. Xu, J. Liu, J. X. He, H. T. Yang, Y. Zeng, Y. Y. He, and C. F. Yang, "Comparison of LR, 5-CV SVM, GA SVM, and PSO SVM for landslide susceptibility assessment in Tibetan Plateau Area, China," Journal of Mountain Science, vol. 20, no. 4, pp. 979-995, 2023. https://doi.org/10.1007/s11629-022-7685-y

[21] Y. Wang, J. Han, and T. Zhang, "A Relief-PGS algorithm for feature selection and data classification," Intelligent Data Analysis, vol. 27, no. 2, pp. 399-415, 2023. https://doi.org/10.3233/IDA-216493

[22] J. Zhou, P. Yang, P. Peng, M. Khandelwal, and Y. Qiu, "Performance evaluation of rockburst prediction based on PSO-SVM, HHO-SVM, and MFO-SVM hybrid models," Mining, Metallurgy & Exploration, vol. 40, no. 2, pp. 617-635, 2023. https://doi.org/10.1007/s42461-022-00713-x

[23] J. Li, J. Shi, Z. Liu, and C. Feng, "A parallel and balanced SVM algorithm on spark for data-intensive computing," Intelligent Data Analysis, vol. 27, no. 4, pp. 1065-1086, 2023. https://doi.org/10.3233/IDA-226774

[24] A. K. Jean, M. A. Diarra, B. A. Bakary, G. O. Pierre, and A. K. Jérôme, "Application based on hybrid CNN-SVM and PCA-SVM approaches for classification of cocoa beans," International Journal of Advanced Computer Science and Applications, vol. 13, no. 9, pp. 231-238, 2022 https://doi.org/10.14569/IJACSA.2022.0130927

[25] S. Samantaray, and D. K. Ghose, "Prediction of S12-MKII rainfall simulator experimental runoff data sets using hybrid PSR-SVM-FFA approaches," Journal of Water and Climate Change, vol. 13, no. 2, pp. 707-734, 2022. https://doi.org/10.2166/wcc.2021.221

[26] X. Zhang, D. Zhao, B. Duan, and W. Qiao, "A novel groundwater burial depth prediction model-based on

the combined VMD-WSD-ELMAN model," Environmental Science and Pollution Research,, vol. 29, no. 50, pp. 76310-76320, 2022. https://doi.org/10.1007/s11356-022-21209-7

[27] P. Zhang, Y. A. Jin, M. Zhang, T. Xi, and L. Xi, "GA-OIHF elman neural network algorithm for fault diagnosis of full life cycle of rolling bearing," Journal of Shanghai Jiaotong University, vol. 55, no. 10, pp. 1255-1262, 2021. https://doi.org/10.16183/j.cnki.jsjtu.2020.157

[28] J. Hao, C. Zhu, and X. Guo, "A new CIGWO-Elman hybrid model for power load forecasting," Journal of Electrical Engineering & Technology, vol. 17, no. 2, pp. 1319-1333, 2022. https://doi.org/10.1007/s42835-021-00928-w

[29] F. Zhang, Y. Kang, X. Cheng, P. Chen, and S. Song, "A hybrid model integrating elman neural network with variational mode decomposition and box-cox transformation for monthly runoff time series prediction," Water Resources Management, vol. 36, no. 10, pp. 3673-3697, 2022. https://doi.org/10.1007/s11269-022-03220-2

[30] X. Xu, X. Wang, K. Li, and Y. Li, "RETRACTED ARTICLE: Source discrimination of mine water inrush based on elman neural network globally optimized by genetic algorithm," Arabian Journal of Geosciences, vol. 14, no. 13, pp. 1204-1213, 2021. https://doi.org/10.1007/s12517-021-06821-0